THE GEOLOGICAL SOCIETY OF AMERICA®

Connections between subducted sediment, pore-fluid pressure, and earthquake behavior along the Alaska megathrust

Jiyao Li[1], Donna J. Shillington[1]*, Demian M. Saffer[2], Anne Bécel[1], Mladen R. Nedimović[3], Harold Kuehn[3], Spahr C. Webb[1], Katie M. Keranen[4], and Geoffrey A. Abers[4]

[1]Lamont-Doherty Earth Observatory of Columbia University, Palisades, New York 10964, USA
[2]Department of Geosciences, The Pennsylvania State University, University Park, Pennsylvania 16802, USA
[3]Department of Earth Sciences, Dalhousie University, Halifax, B3H 4R2 Nova Scotia, Canada
[4]Earth and Atmospheric Sciences, Cornell University, Ithaca, New York 14850, USA

ABSTRACT

Variations in pore-fluid pressure along subduction megathrusts are often invoked to explain differences in fault slip behavior between margins. However, many other parameters vary between subduction zones, making it difficult to isolate the causes of elevated pore fluid pressures and their effects on megathrust behavior. Here we show evidence from pre-stack depth migrations of multichannel seismic reflection data along the subduction zone off the Alaska Peninsula for significant, systematic along-strike variations in the thickness, continuity, P-wave velocity, and estimated pore-fluid pressure of the subducting sediment layer that lines the shallow plate interface within 25 km of the trench. These variations appear to correlate with changes in seismicity, locking, and earthquake rupture history. The currently locked and seismically quiet Semidi segment has a continuous, thick (600–900 m) subducted sediment layer that is characterized by low seismic velocities and elevated pore pressure ($\lambda^* \approx 0.4–0.8$). The subducted sediment in the neighboring Shumagin Gap, a region with low geodetic coupling and abundant small earthquakes, is thinner, irregular and has lower pore pressure ($\lambda^* < 0.2–0.3$). We suggest that the thicker and weakly faulted sediment layer entering the trench at Semidi is associated with a continuous and overpressured sediment layer lining the shallow plate interface, but forms a large coherent asperity as it dewaters and consolidates at greater depths, thus favoring large earthquakes. In contrast, thinner incoming sediment disrupted by outer rise faulting at Shumagin results in a plate interface without elevated pore-fluid pressures, but which is heterogeneous and complex at all depths, contributing to creep and frequent small earthquakes.

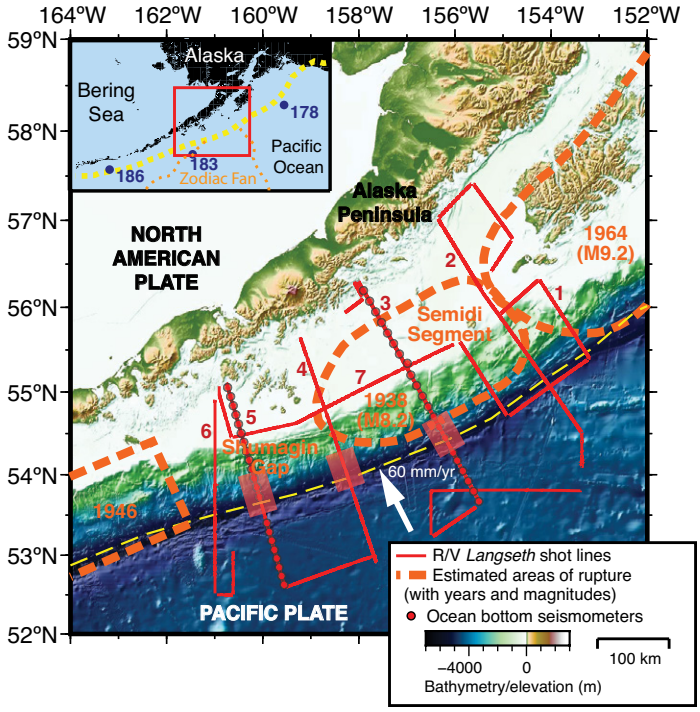

Figure 1. Alaska subduction zone with seismic line locations, estimated rupture areas of large earthquakes (Davies et al., 1981; López and Okal, 2006), and surface trace of plate boundary (dashed yellow line). The near-trench parts of Lines 3, 4, and 5 shown in Figure 2 are marked with transparent red patches. Inset shows the locations of Deep Sea Drilling Program (DSDP) sites (Creager et al., 1973; Kulm et al., 1973) and the extent of the Zodiac fan (Stevenson et al., 1983).

INTRODUCTION

The subduction zone off the Alaska Peninsula (USA) is an ideal locality to examine the impacts of sediments on megathrust properties and slip behavior. Although the thermal structure, convergence rate, obliquity, and plate age remain relatively uniform along strike, the margin exhibits clear variations in present-day seismicity, earthquake rupture history, and megathrust locking (Fig. 1). The Semidi segment is geodetically locked (Fournier and Freymueller, 2007) and has relatively sparse background seismicity (Shillington et al., 2015). It appears to rupture in great earthquakes every 50–75 yr (Davies et al., 1981), most recently as a M8.2 earthquake in A.D. 1938. Previous studies suggest that most slip in the 1938 rupture was relatively deep and generated only a small tsunami (Estabrook et al., 1994; Johnson and Satake, 1994; Lander, 1997). In contrast, the Shumagin Gap is only 30% coupled (Fournier and Freymueller, 2007), has not ruptured in a great earthquake in at least 150 yr (Davies et al., 1981), and exhibits abundant seismicity with M < ~7.0 (Abers et al., 1995; Shillington et al., 2015), particularly at depths of >25 km. Sediment thickness on the incoming plate decreases westward, from >1 km in the Semidi segment to <500 m in the Shumagin Gap, and sediments are increasingly disrupted by outer-rise normal faulting to the west (Shillington et al., 2015), suggesting that the thickness, continuity, and properties of the subducted sediment could contribute to observed variations in slip behavior. Here we quantify along-strike differences in the characteristics of subducting sediments off the Alaska Peninsula with multichannel seismic (MCS) data, use velocities to constrain *in situ* pore fluid pressures, and discuss these observed along-strike variations in the context of megathrust behavior.

*E-mail: djs@ldeo.columbia.edu

SEISMIC DATA ACQUISITION AND ANALYSIS

We analyze three MCS profiles collected during the Alaska Langseth Experiment to Understand the megaThrust (ALEUT) project in 2011 with the R/V *Marcus G. Langseth* that span the Semidi segment and Shumagin Gap (Fig. 1). MCS data were acquired with a 6600 in^3 (108 L) tuned air gun array and an 8-km-long streamer towed at 12 m depth. Coincident wide-angle seismic data were acquired on Lines 3 and 5 with ocean bottom seismometers (OBS) spaced at ~15 km (Fig. 1). We applied Kirchhoff pre-stack depth migration (PSDM) to obtain constraints on the structural configuration and P-wave velocity (Vp) structure of the shallow part of the subduction zone (Fig. 2), where velocities are well-constrained by arrivals on the 8-km streamer. PSDM involves iterative improvement of the velocity model through residual velocity analysis and re-migration. To assess uncertainty in the PSDM-derived velocities, we perturbed the velocity model, re-migrated the data, and assessed the flatness of reflections in the depth-migrated gathers (see the GSA Data Repository[1]).

SEISMIC OBSERVATIONS

We observe dramatic along-strike changes in the thickness and continuity of incoming and subducted sediments and Vp of the subducting sediments (Fig. 2). In the Semidi segment (Line 3), relatively thick sediments are observed on the incoming plate (~1–1.5 km thick), which includes a lower ~800-m-thick layer of distal turbidites from the Eocene-age Zodiac fan, and an upper pelagic sediment layer (Stevenson et al., 1983). Locally, sediment thickness reaches 3 km in the trench due to fill from westward sediment transport along the trench axis (Fig. 2) (e.g., von Huene et al., 2012). The incoming oceanic plate exhibits little normal faulting due to bending (Shillington et al., 2015). The lower part of the incoming section, primarily Zodiac fan sediments, appears to subduct, while the shallower sediments accrete (Fig. 2A).

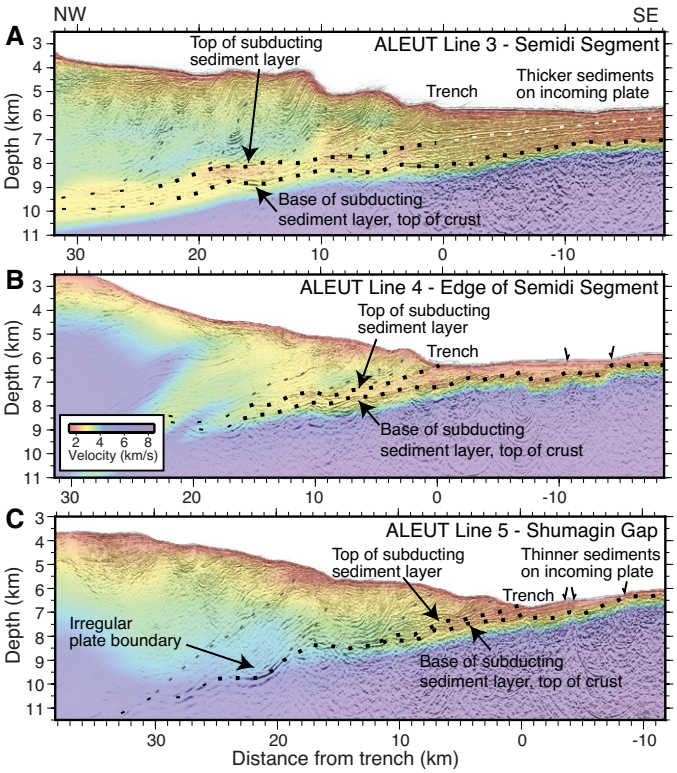

Figure 2. Comparison of the near-trench structure from Lines 3 (A), 4 (B), and 5 (C). Seismic data are overlain on P-wave velocities. Black dashed lines show interpretations. Vertical exaggeration is 2:1.

Landward of the trench, two bright, parallel reflections mark the top and base of a continuous, gently dipping (~4°) subducting sediment layer on Line 3. The thickness of this layer decreases from 900 m at the trench to 600 m by 25 km landward (Fig. 2A). It is associated with a prominent low-velocity zone that persists to at least 25 km from the trench and perhaps as far as 40 km, though it is not well constrained by our data at those depths. The velocity of this layer remains significantly lower than that of the overlying frontal prism, gradually increasing from 2.5 to 3 km/s over 25 km (Figs. 2A and 3A). Uncertainty in the Vp of this layer increases from 5% at the trench to 20% at 25 km from the trench (Fig. 3A). The accretionary prism on Line 3 exhibits features similar to other well-studied accretionary margins, with folded and tilted accreted sediments, and thrust faults that appear to sole out at the plate interface, at the top of the subducting sediment layer (e.g., Bangs et al., 2004).

Farther west, in the Shumagin Gap along Line 5, a thin and irregular incoming sediment section (up to 500 m) is observed on the incoming plate (Fig. 2C), and is disrupted by abundant bending faulting (Shillington et al., 2015). This section is thought to be pelagic in origin (Creager et al., 1973). A thin (<300 m) subducting sediment layer is observed within 5–10 km of the trench with velocities of 2.25 km/s near the trench, increasing to ~3.5 km/s ~10 km from the trench. This layer exhibits velocities slightly lower than the overriding prism (Fig. 2C). Uncertainties in Vp in this layer increase from 5% at the trench to 15% at 10 km. At ~10 km from the trench, a splay thrust fault appears to cut the entire sedimentary section to basement. We interpret this as evidence for the landward termination of most of the subducted section.

Line 4, at the western edge of the Semidi segment, exhibits intermediate features to those along Lines 3 and 5 (Fig. 2B; Li et al., 2015). Clear reflections are observed from the top and base of a low-velocity layer along the plate boundary, though it is thinner (~300–500 m) than on Line 3 and does not persist as far from the trench.

PORE-FLUID PRESSURE ESTIMATES

Vp within the subducting layer along Lines 3 and 4 is substantially lower than in the overlying wedge (Fig. 2), and also lower than expected for its burial depth for the case of hydrostatic pore-fluid pressure (Fig. 3), suggesting the presence of pore-fluid overpressure (Saffer, 2003). Variations in sediment lithology cannot account for differences in velocity. Higher velocities are expected for the distal turbidites of the Zodiac fan subducting in the Semidi segment compared to the pelagic sedimentary section entering the Shumagin Gap, yet the opposite pattern is observed.

To investigate the range of *in situ* pore-fluid pressures that are consistent with the observed velocities, we compare Vp from PSDM analysis along each seismic line with predicted Vp for a range of potential fluid overpressure ratios (see the Data Repository for details). We report fluid pressure as the modified pore pressure ratio, $\lambda^* = (P_f - P_h)/(\sigma_v - P_h)$, where P_f, P_h, and σ_v are the fluid pressure, hydrostatic pressure, and overburden stress, respectively. The ratio $\lambda^* = 0$ for hydrostatic pore pressure, and $\lambda^* = 1$ for lithostatic pore pressure.

We first use the PSDM-derived Vp in the incoming sedimentary section prior to subduction to define a compression trend, which describes the relationship between porosity and vertical effective stress (e.g., Saffer, 2003). We then use the compression trend to compute the expected porosity in the sediment layer with progressive subduction (as a function of distance landward of the trench) for a range of potential values of λ^*. Finally, we predict Vp from the porosity values (Fig. 3) using an empirically determined relationship between Vp and porosity (Hoffman and Tobin, 2004), which fits data for sediments off the Alaska margin drilled during Deep

[1]GSA Data Repository item 2018086, supplemental information and Figures DR1–DR8, is available online at http://www.geosociety.org/datarepository/2018/, or on request from editing@geosociety.org. The study data are available at the Marine Geoscience Data System (http://www.marine-geo.org/tools/new_search/search_map.php).

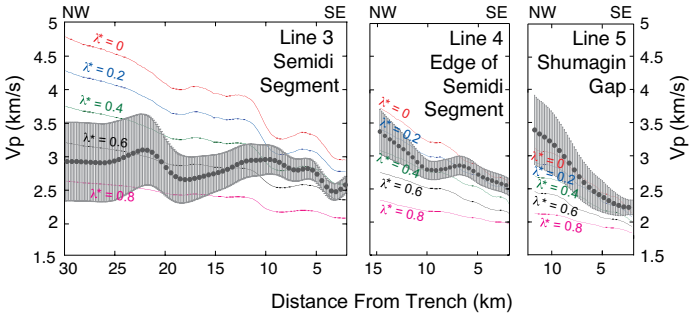

Figure 3. Comparison of observed average velocity in the subducted sediment layer extracted every 180 m (black lines and uncertainty bars) with predicted velocities for different overpressure conditions in the layer (colored lines) for each seismic line, which takes into account variations in overburden in each location.

Sea Drilling Project (DSDP) Legs 18 and 19 (Creager et al., 1973; Kulm et al., 1973; Fig. 1) that sampled the lithologies subducting here.

Comparison between observed and predicted Vp for different pore-fluid pressures reveals substantial variations in pore-fluid pressure within the subducting sediments between transects. Taking into account uncertainties in Vp, the low-velocity sediment layer in the Semidi segment is consistent with λ^* = ~0.4–0.6 within 10 km of the trench, and λ^* = ~0.6–0.8 between 10 and 25 km (Fig. 3A). These values are comparable to overpressures estimated at other sediment-rich subduction zones (e.g., Saffer, 2003). In contrast, Vp in the small, irregular subducting section in the Shumagin Gap is most consistent with that expected for near-hydrostatic pore-fluid pressures ($\lambda^* < 0.2$–0.3; Fig. 3C). The profile at the edge of the Semidi segment (Line 4) exhibits intermediate conditions (Fig. 3B).

DISCUSSION

The observed variations in the thickness, continuity, downdip extent, and estimated pore-fluid overpressure of the subducted sediments across our study area correlate with changes in the thickness and continuity of sediments on the incoming plate. Our analysis suggests higher overpressures along the plate interface in the Semidi segment, where the incoming and subducting sediment is thicker and less disrupted by outer rise faulting (Line 3). This is consistent with the idea that thick, continuous subducting sediments should be associated with higher pore-fluid pressures because their deeper initial burial leads to lower permeability as they are first subducted, and because the path length for upward drainage and dewatering during progressive subduction is longer (Saffer and Bekins, 2006). Shorter drainage paths, especially facilitated by abundant basement irregularities associated with bending faulting as seen on Line 5, would allow lateral drainage as well as vertical dewatering, thus enhancing drainage and leading to lower pore pressures.

The age of the subducting plate and convergence rate do not vary along this part of the subduction zone (Lonsdale, 1988; Sella et al., 2002), and thus along-strike changes in thermal structure and temperature-mediated processes cannot explain observed along-strike patterns in Vp or estimated pore pressure. Limited existing data suggest that the plate interface is expected to be relatively cold (<100 °C) within 30 km of the trench (Batir et al., 2015; Syracuse et al., 2010), so sediment dehydration reactions are not expected here (e.g., Bekins et al., 1994). Consequently, we attribute the formation of significant fluid overpressure in the Semidi segment primarily to disequilibrium compaction. Variations in sediment lithology are also expected in our study area (Creager et al., 1973; Kulm et al., 1973), but they cannot account for estimated variations in pore-fluid pressure. The relatively coarse grained lithologies in the Semidi segment are expected to have higher permeability than the finer grained sediments entering the Shumagin Gap, and thus be less favorable to developing overpressures, but we observe the opposite pattern.

The systematic variations in subducted sediment properties are broadly consistent with patterns of seismicity and megathrust slip behavior along this part of the Alaska margin. Although active deformation is likely focused over a much thinner zone (Rowe et al., 2013) than the >100-m-thick layers constrained by this study and whose properties may vary between and/or during earthquakes (Seno, 2002), our results constrain the average properties around and within the megathrust that can be used to explore possible relationships between plate boundary structure, *in situ* conditions, and earthquake behavior. At shallow depths, the thick, continuous overpressured sediment layer subducting in the Semidi segment, the presence of relatively unconsolidated material in the overlying accretionary prism, and the associated low effective normal stress across the plate interface are likely to favor stable sliding (Scholz, 1998). As the subducting sediment is further buried and consolidates (with concomitant increase in effective vertical stress), it should form a broad and relatively uniform plate interface at greater depths with properties that would allow the nucleation of seismic slip and failure in large earthquakes (Li et al., 2015; Ruff, 1989). This conceptual model is consistent with the observation that the Semidi segment regularly ruptures in great (M > 8) earthquakes, is locked currently, and has little interplate seismicity (Davies et al., 1981). The last great earthquake (M8.2) in the Semidi segment in 1938 is thought to have been a relatively deep rupture (Estabrook et al., 1994; Johnson and Satake, 1994) that generated a small tsunami (Lander, 1997), although a recent paleoseismology study suggests it may have produced a 10-m local tsunami (Nelson et al., 2015). Although our observations suggest that slip may not be favored on the shallow megathrust, coseismic slip on thrusts in the overriding wedge of the Semidi segment could account for large local tsunamis (von Huene et al., 2016). In this region, sediment dewatering and lithification may therefore drive a downdip transition in seismic behavior, as proposed for other sediment-dominated subduction zones (Bangs et al., 2004; Ruff, 1989).

In contrast, the thin, heterogeneous sediment layer subducting in the Shumagin Gap should result in a patchy and geometrically irregular plate interface at all depths, where the plate boundary is mostly creeping (2–30%) and has abundant seismicity (M < ~7.0), particularly at depths >~25 km (Abers et al., 1995; Fournier and Freymueller, 2007). The association of an irregular plate boundary in the Shumagin Gap with creeping behavior is consistent with the idea that heterogeneous stress distribution and fault geometry promote creep along the entire plate boundary (Wang and Bilek, 2014), accompanied by abundant smaller earthquakes. Additionally, the paucity of sediment along the plate boundary and the presence of strong material in the overriding plate close to the trench could suggest that shallow rupture might occur here if, for example, an earthquake that nucleated in the neighboring Semidi section propagated into this segment (Bécel et al., 2017), as may have occurred in A.D. 1788 (Davies et al., 1981).

Our study provides an important test for the long-held idea that subducted sediment thickness is a dominant parameter affecting the pore-fluid pressures in the subducting sediment layers. In addition to the possible impacts described here, differences in plate boundary structure could also influence a host of other processes between and during great earthquakes, including slow slip events and low-frequency earthquakes (e.g., Saffer and Wallace, 2015) and rupture propagation and branching (e.g., Ma and Hirakawa, 2013).

CONCLUSIONS

We document evidence for systematic variations in subducted sediment thickness and pore pressure that correlate with along-strike changes in the thickness and continuity of the incoming sediment section. Changes in effective stress and fault roughness along the plate boundary appear to contribute to different styles of seismic behavior. Where thicker, weakly

faulted sediments subduct, the shallow section is highly overpressured and thus may inhibit shallow earthquake slip on the megathrust. Upon drainage and consolidation at greater depths, these same subducted sediments may promote formation of a large and coherent asperity that exhibits low levels of seismicity but is locked and ruptures regularly in great earthquakes. In contrast, where a thinner, faulted sedimentary section subducts, a heterogeneous plate boundary results, contributing to higher levels of seismicity, creeping behavior, and less regular great earthquakes. These linked observations are consistent with mechanistic models for the roles of effective normal stress and fault roughness in governing megathrust slip behavior and thus hold implications for controls on fault properties and seismic behavior of subduction zones globally.

ACKNOWLEDGMENTS

This project was supported by National Science Foundation grants EAR–1347312, EAR-1347262, OCE–0926614, and OCE-1347343. We thank the Captain, scientific staff, and crew of the R/V *Marcus G. Langseth*. We thank Paradigm (http://www.pdgm.com) for providing seismic data processing software; H. Savage for discussions; and R. Bell, K. Seno, E. Silver, K. Wang, and two anonymous reviewers.

REFERENCES CITED

Abers, G.A., Hu, X., and Sykes, L.R., 1995, Source-scaling of earthquakes in the Shumagin Region, Alaska: time-domain inversions of regional waveforms: Geophysical Journal International, v. 123, p. 41–58, https://doi.org/10.1111/j.1365-246X.1995.tb06660.x.

Bangs, N.L., Shipley, T.H., Gulick, S.P.S., Moore, G.F., Kuromoto, S., and Nakamura, Y., 2004, Evolution of the Nankai Trough décollement from the trench into the seismogenic zone: Inferences from three-dimensional seismic reflection imaging: Geology, v. 32, p. 273–276, https://doi.org/10.1130/G20211.2.

Batir, J., Blackwell, D., and Richards, M., 2015, Heat flow and temperature-depth curves throughout Alaska: Finding regions for future geothermal exploration: Journal of Geophysical Engineering, v. 13, p. 366–377, https://doi.org/10.1088/1742-2132/13/3/366.

Bécel, A., Shillington, D.J., Delescluse, M., Nedimović, M.R., Abers, G.A., Saffer, D., Webb, S.C., Keranen, K.M., Roche, P.-H., Li, J., and Kuehn, H., 2017, Tsunamigenic structures in a creeping section of the Alaska subduction zone: Nature Geoscience, v. 10, https://doi.org/10.1038/ngeo2990.

Bekins, B.A., McCaffrey, A.M., and Dreiss, S.J., 1994, Influence of kinetics on the smectite to illite transition in the Barbados accretionary prism: Journal of Geophysical Research, v. 99, p. 18,147–18,158, https://doi.org/ 10.1029/94JB01187.

Creager, J.S., et. al., 1973, Deep Sea Drilling Project Initial Report, Leg 19: Initial Reports of the Deep Sea Drilling Project, Volume 19:Washington, D.C., U.S. Government Printing Office.

Davies, J., Sykes, L., House, L., and Jacob, K., 1981, Shumagin Seismic Gap, Alaska Penninsula: History of Great Earthquakes, Tectonic Setting, and Evidence for High Seismic Potential: Journal of Geophysical Research, v. 86, p. 3821–3855, https://doi.org/10.1029/JB086iB05p03821.

Estabrook, C.H., Jacob, K.H., and Sykes, L.R., 1994, Body wave and surface wave analysis of large and great earthquakes along the Eastern Aleutian Arc, 1923–1993: Implications for future events: Journal of Geophysical Research, v. 99, p. 11,643–611,662, https://doi.org/10.1029/93JB03124.

Fournier, T.J., and Freymueller, J.T., 2007, Transition from locked to creeping subduction in the Shumagin region, Alaska: Geophysical Research Letters, v. 34, L06303, https://doi.org/10.01029/02006GL029073.

Hoffman, N.W., and Tobin, H.J., 2004, An empirical relationship between velocity and porosity for underthrust sediments in the Nankai Trough accretionary prism, *in* Mikada, H., et al., eds., Proceedings Ocean Drilling Program (ODP) Scientific results, v. 190/196, p. 1–23, http://www-odp.tamu.edu/publications/190196SR/355/355.htm.

Johnson, J.M., and Satake, K., 1994, Rupture extent of the 1938 Alaskan earthquake as inferred from tsunami waveforms: Geophysical Research Letters, v. 21, p. 733–736, https://doi.org/10.1029/94GL00333.

Kulm, L.D., et al., 1973, Initial Reports of the Deep Sea Drilling Project Leg 18: Washington, D.C., U.S. Government Printing Office, https://doi.org/10.2973/dsdp.proc.18.1973.

Lander, J., 1997, Tsunamis affecting Alaska, 1737–1996: Oceanographic Literature Review, v. 6, p. 546–547.

Li, J., Shillington, D.J., Bécel, A., Nedimović, M.R., Webb, S.C., Saffer, D.M., Keranen, K.M., and Kuehn, H., 2015, Downdip variations in seismic reflection character: Implications for fault structure and seismogenic behavior in the Alaska subduction zone: Journal of Geophysical Research, v. 120, p. 7883–7904, https://doi.org/10.1002/2015JB012338.

Lonsdale, P., 1988, Paleogene history of the Kula plate: Offshore evidence and onshore implications: Geological Society of America Bulletin, v. 100, p. 733–754, https://doi.org/10.1130/0016-7606(1988)100<0733:PHOTKP>2.3.CO;2.

López, A.M., and Okal, E.A., 2006, A seismological reassessment of the source of the 1946 Aleutian 'tsunami' earthquakes: Geophysical Journal International, v. 165, p. 835–849, https://doi.org/10.1111/j.1365-246X.2006.02899.x.

Ma, S., and Hirakawa, E.T., 2013, Dynamic wedge failure reveals anomalous energy radiation of shallow subduction earthquakes: Earth and Planetary Science Letters, v. 375, p. 113–122, https://doi.org/10.1016/j.epsl.2013.05.016.

Nelson, A.R., Briggs, R.W., Dura, T., Engelhart, S.E., Gelfenbaum, G., Bradley, L.-A., Forman, S.L., Vane, C.H., and Kelley, K.A., 2015, Tsunami recurrence in the eastern Alaska-Aleutian arc: A Holocene stratigraphic record from Chirikof Island, Alaska: Geosphere, v. 11, p. 1172–1203, https://doi.org/10.1130/GES01108.1.

Rowe, C.D., Moore, J.C., Remitti, F., and Scientists, I.E.T., 2013, The thickness of subduction plate boundary faults from the seafloor into the seismogenic zone: Geology, v. 41, p. 991–994, https://doi.org/10.1130/G34556.1.

Ruff, L.J., 1989, Do trench sediments affect great earthquake occurrence in subduction zones?: Pure and Applied Geophysics, v. 129, p. 263–282, https://doi.org/10.1007/BF00874629.

Saffer, D.M., 2003, Pore pressure development and progressive dewatering in underthrust sediments at the Costa Rican subduction margin: Comparison with northern Barbados and Nankai: Journal of Geophysical Research: Solid Earth, v. 108, B5, https://doi.org/10.1029/2002JB001787.

Saffer, D. M., and Bekins, B. A., 2006, An evaluation of factors influencing pore pressure in accretionary complexes: Implications for taper angle and wedge mechanics: Journal of Geophysical Research v. 111, B04101, https://doi.org/10.01029/02005JB003990.

Saffer, D.M., and Wallace, L.M., 2015, The frictional, hydrologic, metamorphic and thermal habitat of shallow slow earthquakes: Nature Geoscience, v. 8, p. 594–600, https://doi.org/10.1038/ngeo2490.

Scholz, C.H., 1998, Earthquakes and friction laws: Nature, v. 391, p. 37–42, https://doi.org/10.1038/34097.

Sella, G. F., Dixon, T. H., and Mao, A., 2002, REVEL: A model for Recent plate velocities from space geodesy: Journal of Geophysical Research, v. 107, https://doi.org/10:1029/2000JB000033.

Seno, T., 2002, Tsunami earthquakes as transient phenomena: Journal of Geophysical Research, v. 29, https://doi.org/10.1029/2002GL014868.

Shillington, D.J., Bécel, A., Nedimović, M.R., Kuehn, H., Webb, S.C., Abers, G.A., Keranen, K.M., Li, J., Delescluse, M., and Mattei-Salicrup, G.A., 2015, Link between plate fabric, hydration and subduction zone seismicity in Alaska: Nature Geoscience, v. 8, p. 961–964, doi:10.1038/ngeo2586.

Stevenson, A.J., Scholl, D.W., and Vallier, T.L., 1983, Tectonic and geologic implications of the Zodiac fan, Aleutian Abyssal Plain, northeast Pacific: Geological Society of America Bulletin, v. 94, p. 259–273, https://doi.org/10.1130/0016-7606(1983)94<259:TAGIOT>2.0.CO;2.

Syracuse, E.M., van Keken, P.E., and Abers, G.A., 2010, The global range of subduction zone thermal models: Physics of the Earth and Planetary Interiors, v. 183, p. 73–90, https://doi.org/10.1016/j.pepi.2010.02.004.

von Huene, R., Miller, J.J., and Dartnell, P., 2016, A possible transoceanic tsunami directed toward the U.S. West Coast from the Semidi segment, Alaska convergent margin: Geochemistry Geophysics Geosystems, v. 17, p. 645–659, https://doi.org/10.1002/2015GC006147.

von Huene, R., Miller, J.J., and Weinrebe, W., 2012, Subducting plate geology in three great earthquake ruptures of the Western Alaska Margin, Kodiak to Unimak: Geosphere, v. 8, p. 628–644, https://doi.org/10.1130/GES00715.1.

Wang, K.L., and Bilek, S.L., 2014, Invited review paper: Fault creep caused by subduction of rough seafloor relief: Tectonophysics, v. 610, p. 1–24, https://doi.org/10.1016/j.tecto.2013.11.024.

Manuscript received 25 July 2017
Revised manuscript received 27 December 2017
Manuscript accepted 7 January 2018

Printed in USA